Bioanalysis Hot Paper

DOI: 10.1002/anie.201403615

A Supercharged Fluorescent Protein as a Versatile Probe for Homogeneous DNA Detection and Methylation Analysis**

Chunyang Lei, Yan Huang, Zhou Nie, Jun Hu, Lijun Li, Guoyan Lu, Yitao Han, and Shouzhuo Yao*

Abstract: *Supercharged proteins are a new class of functional proteins with exceptional stability and potent ability to deliver bio-macromolecules into cells. As a proof-of-principle, a novel application of supercharged proteins as a versatile biosensing platform for nucleic acid detection and epigenetics analysis is presented. Taking supercharged green fluorescent protein (ScGFP) as the signal reporter, a simple turn-on homogenous method for DNA detection has been developed based on the polyionic nanoscale complex of ScGFP/DNA and toehold strand displacement. This assay shows high sensitivity and potent ability to detect single-base mismatch. Furthermore, combined with bisulfite conversion, this ScGFP-based assay was further applied to analyze site-specific DNA methylation status of genomic DNA extracted from real human colon carcinoma tissue sample with ultrahigh sensitivity (4 amol methylated DNA).*

Biomolecular detection with high sensitivity, selectivity, simplicity, and cost-efficiency is significant and desirable in clinical diagnosis, drug discovery, and environmental analysis. Functional proteins, such as fluorescent proteins and immunoglobulins, are valuable in the development of bio-detection methods. Supercharged proteins (ScP) have emerged as a new class of functional proteins with high surface net charge.[1] Recently, a new kind of ScP, namely supercharged green fluorescent protein (ScGFP), was developed by Liu et al. by resurfacing green fluorescent protein by genetic modification.[2] As protein aggregation causes major problems in biotechnology and many fatal human diseases, ScP shows exceptional solubility and stability against protein aggregation, exhibiting great promise for applications in biotechnology, medicine, and material science.[3] Moreover, supercharged proteins are cell penetrating and are able to efficiently deliver functional nucleic acid and protein into mammalian cells.[4] These ScPs possess several advantages over conventional delivery vectors, including low cytotoxicity, high versatility, and generality across various cell types.[4a] The self-assembled polyionic complex is formed by electrostatic interaction between superpositive ScP and negatively charged nucleic acid, which is similar to the natural assembly of histone protein and oppositely charged DNA. Owing to their robust stability, cell penetrating ability, and strong electrostatic interaction with nucleic acid, it will be attractive to adopt ScP as a biosensing platform. However, the application of ScPs in bio-detection is scarce. Herein, taking ScGFP with a net charge of +36 as the signal reporter, we demonstrate ScP as a simple and versatile platform for genetic diagnosis and epigenetics analysis. The homogenous detection of DNA mutation and methylation analysis of cancer tissue samples are achieved.

Scheme 1 shows the detection mechanism for this ScGFP-based platform. The strong electrostatic interaction between +36 ScGFP and DNA leads to assembly of a polyionic nanoscale complex. As the DNA tailed with the organic quencher BHQ1, the close proximity between BHQ1-DNA and ScGFP in the nanoscale complex results in highly efficient quenching of ScGFP fluorescence by energy transfer (Supporting Information, Figure S1). The ScGFP fluorescence can be restored by releasing the quencher from DNA and distancing it from ScGFP. Based on this principle, homogenous DNA detection has been developed straightfor-

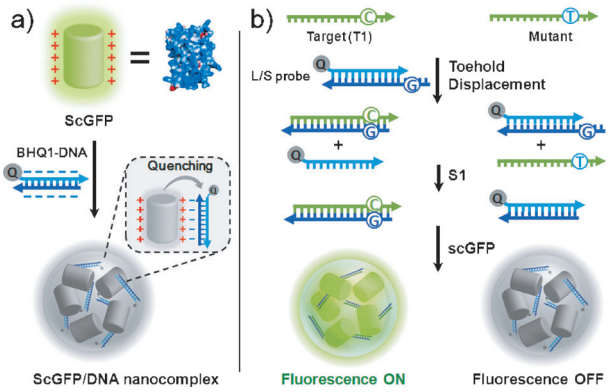

Scheme 1. Representation of the ScGFP-based sensing platform. a) Interaction between ScGFP and DNA. b) Homogenous DNA fluorescence assay.

[*] C. Y. Lei, Dr. Y. Huang, Prof. Dr. Z. Nie, L. J. Li, G. Y. Lu, Y. T. Han, Prof. Dr. S. Z. Yao
State Key Laboratory of Chemo/Biosensing and Chemometrics
College of Chemistry and Chemical Engineering
Hunan University, ChangSha 410082 (P.R. China)
E-mail: niezhou.hnu@gmail.com

J. Hu
Pathology Department of Hunan Provincial Tumor Hospital/
the Affiliated Tumor Hospital of Xiangya Medical School
Central South University, Changsha, Hunan 410013 (China)

[**] We are grateful to the National Natural Science Foundation of China (Nos. 21222507, 21175036, 21235002, and 21190044), the National Basic Research Program of China (973 Program, No. 2011CB911002), and the Foundation for Innovative Research Groups of NSFC (Grant 21221003).

Supporting information for this article is available on the WWW under http://dx.doi.org/10.1002/anie.201403615.

wardly. A BHQ1-tagged toehold DNA probe, comprising a long (L) strand and a short (S) strand, is applied. Target DNA (T1), which is totally complementary to L of the probe, can hybridize with single-stranded toehold region of the L-S probe and then initiate the toehold-mediated strand displacement,[5] which consequently releases the BHQ1-tagged S. The single-strand specific nuclease, S1 nuclease, is sequentially introduced to cleave S completely to liberate quencher and retain the T1L duplex. The nanoscale complex formed by quencher-free T1L and ScGFP induces the fluorogenic signal-out. Conversely, in the presence of mutant target or without target DNA, the S1-treated probe duplex still contains BHQ1 owing to lack of strand displacement, leading to significant fluorescence quenching by combination with ScGFP. As a result, this signal-on design provides a quantitative fluorescence measurement of the target DNA.

As the nanoscale complex formed by electrostatic interaction between ScGFP and DNA is essential for efficient quenching, the ScGFP/DNA nanoscale complex was investigated first. Using +36 ScGFP and 20 bp double-stranded DNA (dsDNA)-BHQ1 (ds20-Q) as models, the fluorescence titration experiment (Figure 1a) showed that the fluorescence

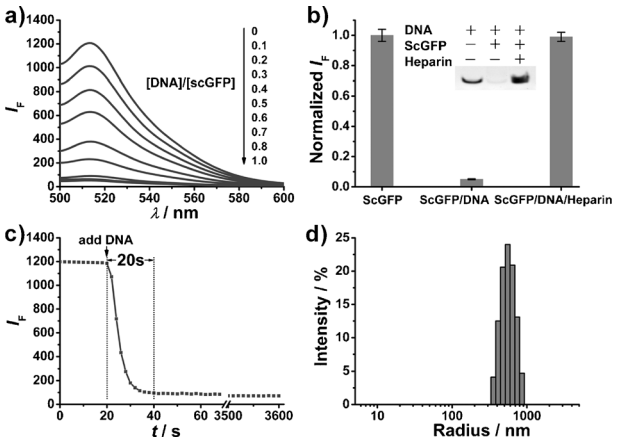

Figure 1. a) Fluorescence spectra of ScGFP (100 nM) in the presence of ds20-Q with varying [DNA]/[ScGFP] ratios. b) Normalized fluorescence intensity of ScGFP, ScGFP/ds20-Q, and ScGFP/ds20-Q/heparin in the buffer solution. Inset: gel electrophoresis images of heparin competition using ds20. c) Kinetic study of fluorescence change of ScGFP after addition of ds20-Q (100 nM). d) DLS data revealing the size distribution of ScGFP/DNA complex.

gradually decreased with increasing concentration ratio of DNA to ScGFP (D/S) and reached quenching saturation at about 0.8/1 D/S with maximal quenching rate of 95%, indicating the complete assembly of nanoscale complex. This fluorescence result was validated by electrophoretic mobility assay (Supporting Information, Figure S2), and the band of 20 bp DNA significantly faded at 1/1 D/S and completely disappeared at 1/2 D/S, demonstrating that the DNA is totally bound by ScGFP to form a nanoscale complex. In contrast, ds20-Q showed no quenching effect on the enhanced GFP (EGFP, a non-supercharged control) owing to no complexation of EGFP with DNA (Supporting Information, Figure S3). Increasing the concentration of sodium chloride to 0.4 M (Supporting Information, Figure S4) or the addition of heparin (a polyanionic competitor, 0.025% m/v, Figure 1b) could completely restore the fluorescence of ScGFP, respectively, proving that the nanoscale complex is formed by electrostatic interaction. The ScGFP/DNA nanoscale complex generated very quickly (in 20 s; Figure 1c) with an average diameter of 568 ± 46 nm, which was characterized by dynamic light scattering (DLS; Figure 1d), and its formation was further demonstrated by atomic force microscopy (Supporting Information, Figure S5). Moreover, the fluorescence quenching rate of nanoscale complex remained stable as long as one hour (Figure 1c), suggesting that this nanoscale complex is stable. According to the DNA concentration-dependent quenching curve, the dissociation constant value (K_d) of 0.33 nM between ScGFP and 20 bp dsDNA could be estimated by using nonlinear least-squares curve-fitting analysis (as shown in the Supporting Information).[6] Further examination of the ScGFP/DNA nanoscale complex (Supporting Information, Figure S6) indicated that both single-stranded DNA (ssDNA) and dsDNA with BHQ1 can efficiently quench the fluorescence of ScGFP. For quenching efficiency, ssDNA was marginally better than dsDNA and short strands were slightly more efficient than long strands, which are probably due to that each DNA sample with the same total charge contains different amount of quencher. The maximal quenching rate was up to 99% obtained by 8 nt ssDNA, implying that the quenching of ScGFP by multiple proximate quenchers in polyionic nanoscale complex is highly efficient. Interestingly, the nanoscale complex of ScGFP with quencher-free DNA caused an almost 50% fluorescence increase, which is probably due to the surrounding environment change and confined state of ScGFP in nanoscale complex (Supporting Information, Figure S7). The fluorescence stability of this nanoscale complex was also investigated. It was found that the BHQ1-free ScGFP/DNA nanoscale complex maintained over 95% of its initial fluorescence after two hours (Supporting Information, Figure S8a). Additionally, the fluorescence anisotropy of ScGFP decreased significantly from 0.3 to 0.07 after being encapsulated in nanoscale complex, which could be reasoned by the homo-FRET among ScGFP molecules in ScGFP/DNA complex (Supporting Information, Figure S8b).[7] The formation of quencher-free ScGFP/DNA nanoscale complex can be directly observed by confocal fluorescence microscopy (Supporting Information, Figure S9).

Based on the efficient fluorescence quenching of ScGFP by DNA-mediated nanoscale complex formation, the quantitative DNA analysis was performed using the toehold DNA probe (L-S, detailed sequences are shown in the Supporting Information, Table S1) with BHQ1. The target (T1) is derived from the segment of human *TP53* gene encoding a crucial tumor suppressor protein p53.[8] As the concentration of T1 increased, the fluorescence of ScGFP monotonically intensified and almost reached saturation with 200 nM T1 (Figure 2a). In the presence of 200 nM T1, the fluorescence intensity increased by 14.7 times as compared with the probe-only control, demonstrating that our ScGFP-based sensor is feasible for DNA detection. It is noteworthy that the high

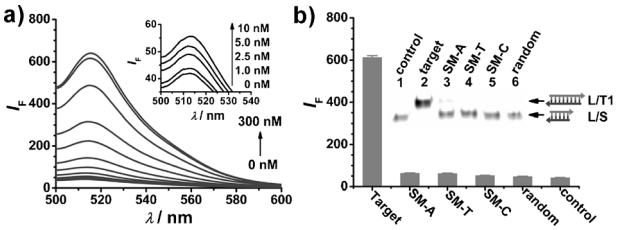

Figure 2. a) Fluorescence responses of ScGFP-based assay to varying concentrations of *TP53* target (T1). Inset: Responses at low T1 concentrations. b) Fluorescence responses to target T1, SMs, random sequence, and probe-only. Inset: gel electrophoresis of probe (non-labeled) and probe/sample hybrids after S1 digestion. Lane 1: the probe; lanes 2–6: the hybrids of probe/target(C/G), probe/SM-A (C/A), probe/SM-T (C/T), probe/SM-C (C/C), and probe/random, respectively. [ScGFP] = 100 nM, [L/S probe] = 100 nM.

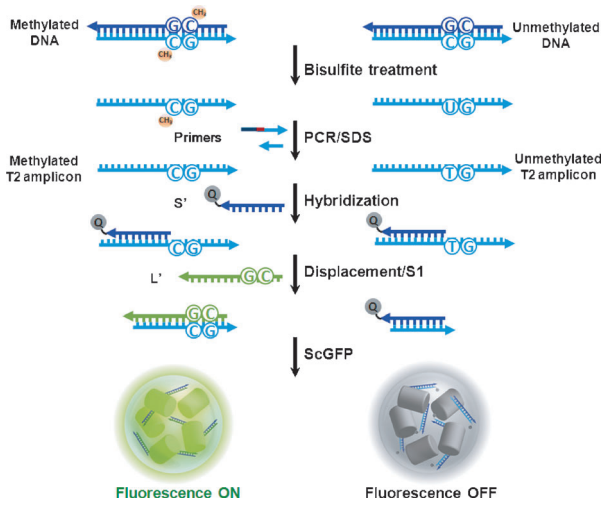

Scheme 2. ScGFP-based DNA methylation assay.

signal-to-background (S/B) ratio of above 14 is much better than that of conventional homogenous fluorescent protein-based sensors.[9] According to the relative calibration curve (Supporting Information, Figure S10), the ScGFP-based sensor shows a linear response in the range from 1 to 100 nM with the lowest detectable concentration of 1 nM, which is better than many nanomaterials-based homogenous methods (Supporting Information, Table S3).[10]

The selectivity of this sensor was examined by testing its response toward T1 and a series of single-base mismatched sequences (SMs). Herein, the mutation hotspot R273H of *TP53* gene was included in T1 and its SMs were tested (Figure 2b). The signal intensity of the sensor in response to 200 nM target was 9.7, 9.9, and 11.8 times that responsive to the same concentration of C/A, C/T, and C/C SMs, respectively. The gel electrophoresis experiments also demonstrated the high specificity of this sensor (inset of Figure 2b), because the SMs cannot efficiently displace the S strand in the toehold probe.[11] The significant fluorescence difference (ca. 10-fold) implied the potency of ScGFP-based DNA sensor to discriminate SMs, and its sequence specificity is better than the single base extension method,[12a] molecular beacons,[12b] invasive cleavage probes,[12c] and many nanomaterials-based methods (Supporting Information, Table S3).[10a–d,13]

The good S/B ratio and great specificity to discriminate the single-base mutations of this ScGFP-based biosensor motivated us to explore its advanced application in epigenetic analysis. DNA methylation is an essential epigenetic mechanism for cellular regulation of gene expression.[14] In mammalian cells, DNA methylation occurs by addition of a methyl group to the 5-position of cytosine almost exclusively within the CpG site.[14a] Aberrant DNA methylation is recognized as the earliest and most common event in carcinogenesis.[14b] Bisulfite treatment of DNA converts cytosine (C) into uracil (U) while leaving methylcytosine (mC) unaltered, which is well-recognized as an efficient recognition mechanism for DNA methylation.[15] Considering the bisulfite treatment-induced one base alternation between mC and C, we expected to integrate bisulfite treatment and the ScGFP-based DNA sensing platform to develop a novel method to detect DNA methylation. Scheme 2 outlines the mechanism of ScGFP-based DNA methylation detection. Treatment of genomic DNA by sodium bisulfite leads to conversion of C to U, which is subsequently replicated as thymine (T) during PCR amplification of target DNA loci of interest, while mC is resistant to deamination and is replicated as C during amplification. One of the primers for PCR is rationally designed by introduction of a nicking site for further ssDNA target preparation. With the assistance of nicking enzyme Nb.BbvCI and DNA polymerase, the PCR product serves as a template to prepare target ssDNA amplicon (T2) by nicking enzyme-mediated strand displacement synthesis (SDS). Finally, the resulting T2 with methylation-induced C/T alternation at CpG site is measured by the modified ScGFP-based probing process (the reason for using the modified process is discussed in the section "Detection of site-specific CpG methylation" in the Supporting Information). Similarly, a pair of long and BHQ-1-tagged short (L′ and S′, sequence shown in the Supporting Information, Table S2) DNA strands are used as the probe. In this case, both L′ and S′ are complementary to T2. S′ can pair with downstream sequence next to the CpG site. L′ is 5 nt longer than S′ and the elongation part of L′ can hybridize with CpG site and its upstream sequence of the methylated T2 (meT2) to initiate toehold-mediated strand displacement of S′. However, for the unmethylated T2 (umT2), strand displacement is prohibited because of one-base mismatch of L′ to TpG site. After S1 cleavage, the meT2 complementary to L′ yields a quencher-free L′-T2 duplex while umT2 causes negligible strand displacement and leaves a quencher-containing S′-T2 duplex. The addition of ScGFP results in the fluorescence light-on for methylated sample and light-off for unmethylated one, achieving a signal-on detection of DNA methylation.

The target of interest is the methylation status of the CpG site in the promoter region of *p16* tumor-suppressor gene.[16] Plasmid pUC19 containing *p16* promoter sequence, which was fully methylated by M.SssI methyltransferase, serves as the methylation-positive sample. The negative control was the unmethylated plasmid. After bisulfite conversion, the amplicon T2 was generated by PCR and the subsequent SDS, and

the gel electrophoresis analysis (Supporting Information, Figure S11) of replication products demonstrates the highly efficient target amplification and the dominant yield of single-stranded product. Besides the methylation probe (Me probe) with L′ complementary to meT2, we also designed another counterpart probe (non-Me probe) specific for umT2 to double check the methylation status of interested locus and to avoid false positives. As shown in Figure 3a, with respect to

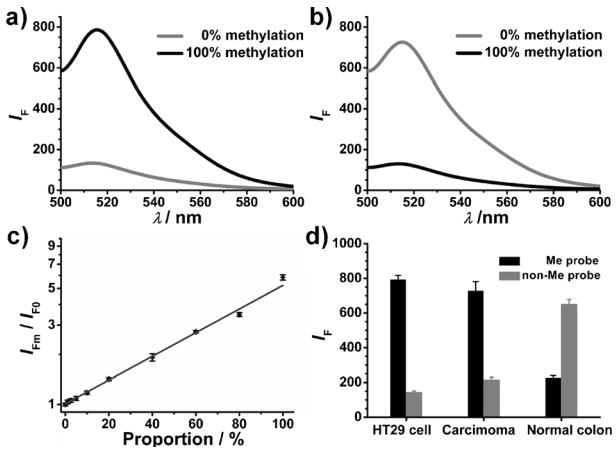

Figure 3. Fluorescence responses of ScGFP-based assay to methylated DNA and unmethylated DNA using a) Me probe and b) non-Me probe. c) Fluorescence responses with various proportions of methylated DNA using Me probe. I_{F0} and I_{Fm} are fluorescence intensity in response to unmethylated DNA and varying proportions of methylated DNA, respectively. d) Fluorescence detection of methylation status of *p16* promoter in human cancer cell line HT29, human colon carcinoma tissue and normal colon tissue using Me probe and non-Me probe, respectively. [ScGFP] = 100 nM, [S′] = 80 nM, and [L′] = 320 nM.

the Me probe, the fluorescence signal of full methylated plasmid was 5.9 times higher than that of unmethylated one. Correspondingly, the unmethylated sample showed 5.7 times the fluorescence intensity of methylated one in case of the non-Me probe (Figure 3b). The remarkable signal response indicated that our new method is specific for methylation of CpG loci. The good specificity is due to the toehold-displacement susceptible to one base mismatch, which was confirmed by gel electrophoresis analysis of DNA probe (Supporting Information, Figure S12). For quantitative measurement of DNA methylation, the fluorescence signal of the proposed assay in response to different methylation proportions was investigated. The increasing methylation proportion induced the increase of fluorescent signal (I_{Fm}) of Me probe-based assay (Figure 3c; Supporting Information, Figure S13a) and the decrease of fluorescent signal (I_{Fn}) of the assay using non-Me probe (Supporting Information, Figure S14), respectively. It demonstrated that even low level of methylation (1%; Supporting Information, Figure S13b) can be detected by our assay. This method was highly sensitive with the detection limit of 4 amol methylated DNA, which is lower than some conventional methods (Supporting Information, Table S4).[17] As a result, our method can serve as a potent technique to probe DNA methylation status specifically and quantitatively.

This method was further used to determine the methylation status of CpG island in the *p16* promoter region of human colon cancer cell line HT29 and real human colon carcinoma tissue sample. Colon cancer is one of the most aggressive malignancies and occurs at a high incidence in most countries. The *p16* inactivation caused by aberrant hyper-methylation of its promoter was significantly associated with colorectal tumorigenesis.[18] The genomic DNA extracted from the cancer cells underwent bisulfite conversion and then the nested-PCR amplification was performed to specifically amplify the target sequence containing CpG island. The highly efficient preparation of ssDNA target amplicon was confirmed by gel analysis (Supporting Information, Figure S15). The examined HT29 cell line exhibited significant fluorescence signal of Me probe, which was 5.7 times more than that of non-Me probe (Figure 3d), indicating the CpG site of interest is heavily methylated in the colon cancer cell. The comparative methylation analysis of colon carcinoma tissue and normal colon tissue was carried out for real sample analysis. The signal ratio of dual probes (I_{Fm}/I_{Fn}) for colon carcinoma tissue and normal tissue were 3.4 and 0.35, respectively (Figure 3d). According to the calibration curve of I_{Fm}/I_{Fn} (Supporting Information, Figure S16), the methylation level of HT29 cells, carcinoma tissue, and normal colon tissue were estimated as 99.6, 85.2, and 18.6%, respectively, which were comparable with the results of bisulfite sequencing (Supporting Information, Figure S17). These results verified that *p16* hypermethylation specifically occurs in the tumor tissue. All these results prove that our method provides a potential technique for DNA methylation-related clinical diagnosis of cancer.

In summary, we exploited the supercharged protein to develop a simple and versatile fluorescence platform for homogenous DNA detection and methylation analysis of specific gene loci. This biosensor, relying on the highly efficient quenching of ScGFP/DNA-quencher nanoscale complex and toehold-mediated strand displacement, exhibits great specificity, sensitivity, and general applicability in DNA detection and methylation assay. Unlike conventional fluorescent protein-based biosensor, the ScGFP probe preparation is convenient and low-cost without the requirement of further genetic fusion and engineering. The successful determination of DNA methylation levels in real tumor tissue indicates that the system is promising for future application in epigenetic analysis and cancer diagnosis. Considering the intriguing cell penetrating and DNA carrying abilities of ScGFP, it is expected that this ScGFP-based strategy can be further improved to achieve intracellular detection of important target biomolecules. The present study provides a new function of highly promising biomaterials, namely supercharged proteins, as a nucleic acid biosensor, which will inspire the exploration of more widespread applications of these emerging functional proteins.

Received: March 23, 2014
Published online: June 24, 2014

Keywords: bioanalysis · DNA · DNA methylation · supercharged protein · toehold strand displacement

[1] a) D. B. Thompson, J. J. Cronican, D. R. Liu, *Methods Enzymol.* **2012**, *503*, 293; b) J. J. Cronican et al., *Chem. Biol.* **2011**, *18*, 833.
[2] M. S. Lawrence, K. J. Phillips, D. R. Liu, *J. Am. Chem. Soc.* **2007**, *129*, 10110.
[3] a) M. Vendruscolo, C. M. Dobson, *Nature* **2007**, *449*, 555; b) A. E. Miklos et al., *Chem. Biol.* **2012**, *19*, 449.
[4] a) B. R. McNaughton, J. J. Cronican, D. B. Thompson, D. R. Liu, *Proc. Natl. Acad. Sci. USA* **2009**, *106*, 6111; b) J. J. Cronican, D. B. Thompson, K. T. Beier, B. R. McNaughton, C. L. Cepko, D. R. Liu, *ACS Chem. Biol.* **2010**, *5*, 747.
[5] B. B. Li, Y. Jiang, X. Chen, A. D. Ellington, *J. Am. Chem. Soc.* **2012**, *134*, 13918.
[6] C. C. You, M. De, G. Han, V. M. Rotello, *J. Am. Chem. Soc.* **2005**, *127*, 12873.
[7] a) A. N. Bader, S. Hoetzl, E. G. Hofman, J. Voortman, P. M. P. van Bergen en Henegouwen, G. van Meer, H. C. Gerritsen, *ChemPhysChem* **2011**, *12*, 475; b) F. T. S. Chan, C. F. Kaminski, G. S. Kaminski Schierle, *ChemPhysChem* **2011**, *12*, 500.
[8] A. Petitjean, M. I. W. Achatz, A. L. Borresen-Dale, P. Hainaut, M. Oliver, *Oncogene* **2007**, *26*, 2157.
[9] a) E. M. van Dongen, T. H. Evers, L. M. Dekkers, E. W. Meijer, L. W. Klomp, M. Merkx, *J. Am. Chem. Soc.* **2007**, *129*, 3494; b) L. W. Nausch, J. Ledoux, A. D. Bonev, M. T. Nelson, W. R. Dostmann, *Proc. Natl. Acad. Sci. USA* **2008**, *105*, 365.
[10] a) R. H. Yang, J. Y. Jin, Y. Chen, N. Shao, H. Z. Kang, Z. Y. Xiao, Z. W. Tang, Y. R. Wu, W. H. Tan, *J. Am. Chem. Soc.* **2008**, *130*, 8351; b) C. H. Lu, H. H. Yang, C. L. Zhu, X. Chen, G. N. Chen, *Angew. Chem.* **2009**, *121*, 4879; *Angew. Chem. Int. Ed.* **2009**, *48*, 4785; c) H. F. Dong, W. H. Gao, F. Yan, H. X. Ji, H. X. Ju, *Anal. Chem.* **2010**, *82*, 5511; d) L. B. Zhang, S. J. Guo, S. J. Dong, E. K. Wang, *Anal. Chem.* **2012**, *84*, 3568; e) Q. B. Wang, W. Wang, J. P. Lei, N. Xu, F. L. Gao, H. X. Ju, *Anal. Chem.* **2013**, *85*, 12182.
[11] a) D. Y. Zhang, S. X. Chen, P. Yin, *Nat. Chem.* **2012**, *4*, 208; b) Y. S. Jiang, S. Bhadra, B. L. Li, A. D. Ellington, *Angew. Chem.* **2014**, *126*, 1876; *Angew. Chem. Int. Ed.* **2014**, *53*, 1845.
[12] a) X. R. Duan, Z. P. Li, F. He, S. Wang, *J. Am. Chem. Soc.* **2007**, *129*, 4154; b) Y. V. Gerasimova, S. Hayson, J. Ballantyne, D. M. Kolpashchikov, *ChemBioChem* **2010**, *11*, 1762; c) M. R. Lockett, M. R. Shortreed, L. M. Smith, *Anal. Chem.* **2007**, *79*, 6031.
[13] a) L. B. Zhang, J. B. Zhu, S. J. Guo, T. Li, J. Li, E. K. Wang, *J. Am. Chem. Soc.* **2013**, *135*, 2403; b) S. P. Song, Z. Q. Liang, J. Zhang, L. H. Zhang, L. H. Wang, G. X. Li, C. H. Fan, *Angew. Chem.* **2009**, *121*, 8826; *Angew. Chem. Int. Ed.* **2009**, *48*, 8670.
[14] a) K. D. Robertson, A. P. Wolffe, *Nat. Rev. Genet.* **2000**, *1*, 11; b) P. W. Laird, *Nat. Rev. Genet.* **2010**, *11*, 191.
[15] M. Frommer, L. E. McDonald, D. S. Millar, C. M. Collis, F. Watt, G. W. Grigg, P. L. Molloy, C. L. Paul, *Proc. Natl. Acad. Sci. USA* **1992**, *89*, 1827.
[16] J. G. Herman, A. Merlo, L. Mao, R. G. Lapidus, J. P. Issa, N. E. Davidson, D. Sidransky, S. B. Baylin, *Cancer Res.* **1995**, *55*, 4525.
[17] a) J. Tost, P. Schatz, M. Schuster, K. Berlin, I. G. Gut, *Nucleic Acids Res.* **2003**, *31*, e50; b) A. H. Badran, J. L. Furman, A. S. Ma, T. J. Comi, J. R. Porter, I. Ghosh, *Anal. Chem.* **2011**, *83*, 7151; c) R. Kurita, K. Arai, K. Nakamoto, D. Kato, O. Niwa, *Anal. Chem.* **2012**, *84*, 1799; d) J. Hu, C. Y. Zhang, *Biosens. Bioelectron.* **2012**, *31*, 451; e) X. L. Wang, Y. L. Song, M. Y. Song, Z. X. Wang, T. Li, H. L. Wang, *Anal. Chem.* **2009**, *81*, 7885.
[18] a) V. V. Lao, W. M. Grady, *Nat. Rev. Gastroenterol. Hepatol.* **2011**, *8*, 686; b) F. J. Carmona, M. Esteller, *Mutat. Res.* **2010**, *693*, 53.

